

RESEARCH ARTICLE

WILEY

Performance enhancement of UWA-OFDM communication systems based on FWHT

Mohamed El-Mahallawy¹ | Adly Tag Eldien²

¹Department of Electronics and Electrical Communications, Higher Institute of Engineering, El-Shorouk Academy, Cairo, Egypt

²Department of Electronics and Electrical Communications, Faculty of Electronic Engineering, Benha University, Shoubra, Egypt

Correspondence

Mohamed El-Mahallawy, Department of Electronics and Electrical Communications, Higher Institute of Engineering, El-Shorouk Academy, Cairo, Egypt.
Email: mohmedmahallawy@gmail.com

Summary

The available bandwidth of underwater environment tends to several kilohertz, which considers the main challenges of communications under sea water. On the other hand, the bit-error-rate (BER) performance degrades because of several reasons such as multipath propagation, time variabilities of the channel, attenuation, and water temperature. In this paper, we aim to improve the underwater acoustic (UWA) BER system performance by using orthogonal frequency division multiplexing (OFDM) based on fast Walsh-Hadamard transform (FWHT) instead of fast Fourier transform (FFT). We proposed a low-complexity equalization and carrier frequency offset (CFO) compensation for UWA-OFDM-based FWHT using banded-matrix approximation concept. Simulation results show that the UWA-OFDM-based FWHT with low-density parity check (LDPC) codes give a good improvement performance compared with traditional OFDM in UWA system especially in case of estimation errors.

KEYWORDS

FFT, FWHT, LDPC, OFDM, UWA

1 | INTRODUCTION

The underwater acoustic (UWA) communication systems support significantly low data rate¹ due to large delay spread and limited the available bandwidth (BW). The UWA channel has a lot of challenges such as attenuation, water salinity, temperature, frequency-dependent attenuation, and time-varying nature. Thus, those challenges cause a limitation to communications in sea water.² In general, the ocean water can be divided into four horizontal layers: the surface layer (mixed layer), seasonal thermocline layer, permanent thermocline layer, and deep isothermal layer. The sound propagation speed differs in each layer because of the variation of the water properties (salinity, pressure, and temperature).³ The propagation speed differs in each layer according to the water properties (temperature, salinity, and water depth). To establish the communication over the underwater environment, four different communication media have been used. Cables are not suitable to establish the underwater communications (not realistic). The electromagnetic and optical waves support a range that does not exceed 100 m because of the large power loss.¹ Thus, we are forced to use sound waves. Moreover, acoustic waves support a frequency ranging up to tens of kilohertz. The main advantages of the use of acoustic waves are the lower power loss and effective range reaches to several kilometers, and the disadvantage is the low propagation speed (1500 m/s).

The orthogonal frequency division multiplexing (OFDM) modulation is a type of modulation that can be used for UWA communications⁴⁻⁷. The OFDM communication systems suffer from two main performance degradation: the

peak-to-average power ratio (PAPR) at the transmitter side⁸ and the carrier frequency offset (CFO) at the receiver side.⁹ The PAPR results from the limited range of the power amplifier; moreover, the PAPR increases as the number of subcarriers increased. There are different algorithms used for PAPR reduction such as in previous studies.⁸⁻¹¹ On the other hand, the CFO results from the relative motion of the transmitter and/or receiver (Doppler effect).¹² The CFO induces intercarrier interference (ICI), which destroys the orthogonality and consequently degradation in the bit-error-rate (BER) performance.^{13,14} There are different algorithms used for CFO estimations such as in previous works.¹⁵⁻¹⁹ The OFDM system lies in its simplicity by using a frequency domain equalizer (FDE) at the receiver side to mitigate the intersymbol interference (ISI) effect and improve the system performance. In the same time, we modify the OFDM system by replacing the inverse fast Fourier transform (IFFT) and fast Fourier transform (FFT) by inverse fast Walsh-Hadamard transform (IFWHT) and fast Walsh-Hadamard transform (FWHT), respectively. Replacing the FWHT/IFWHT with FFT/IFFT has been introduced in wireless radio communications,²⁰ which can improve the system performance.²⁰ But this modification requires an FFT and IFFT block to implement the FDE and enhance the system performance when compared with traditional OFDM system. On the other hand, implementation of the FWHT requires fewer computations (it omits the FFT's twiddle factors), and implement on smaller and cheaper hardware can be used to improve the performance of the UWA communication system and give better data transmission.²¹ The FWHT transform can be implemented with lower complexity, due to its operation that is built on the subtraction and addition operations, while the FFT transform requires multiplication and division.²² Also, the FWHT can be used for channel estimation with lower complexity.²² Yang and Yang²³ show that the FWHT can be highly attentive to deal with the UWA channel impairments, and it is built on removing the interference using an algorithm called hyperspace cancellation by coordinate zeroing. The drawback of using FWHT is the time synchronization. Our proposed structure uses the Zadoff-Chu (ZC) sequences to compensate the effect of symbol time offset (STO),¹⁷ knowing that the ZC sequences have the ability to make an STO in the presence of CFO.¹⁷

There are different coding algorithms used to improve the system performance such as turbo codes.^{24,25} The turbo codes are originally developed for decoding.²⁶ The channel estimation based on turbo equalization has been studied in UWA communication systems.²⁷⁻²⁹ The turbo codes are used for channel coding in UWA communication systems³⁰ and give the improvement in the BER performance.²⁹ The low-density parity check (LDPC) codes are used for UWA communication systems.³¹ Moreover, the LDPC codes give a superior to the BER performance compared with turbo coding.^{32,33} The LDPC codes have been presented by Gallager in 1962 and 1963.^{34,35} It is a kind of a special linear block code that depends on parity check matrix (H) or generator matrix (G). The H matrix contains law number of 1's to satisfied the conditions of $\gamma \ll m$ and $\rho \ll n$, where γ and ρ represent the number of 1's per each column and row, respectively. The number of 1's in each row and column of H is called row and column weights. The code is named regular LDPC code if row and column weights are fixed. The code is named irregular LDPC code if row weight or column weight is infixed.³³

Equalization is one of the most used algorithm to improve the UWA-OFDM system performance.^{2,36-39} The zero forcing (ZF) equalizer can be used for channel equalization; this type of equalizer suffers from noise enhancement. The minimum mean square error (MMSE) equalizer can mitigate the noise enhancement, but this type of equalizer suffers from high complexity and requires the estimation of the signal-to-noise ratio (SNR) to work probably.⁴⁰ In this paper, we propose an MMSE equalizer that performs the equalization and the CFO compensation processes jointly with low complexity using banded matrix approximation.⁴¹ The main differences between the proposed structure and those of previous studies^{22,23,42} are that our proposed structure can perform a time synchronization using the ZC sequences, and the equalization and CFO compensation processes can be preformed jointly with low complexity using banded matrix approximation.⁴¹

This paper presents a modified OFDM with LDPC codes for UWA-OFDM systems based on FWHT and compared its performance with traditional OFDM system. This paper is organized as follow: The modified UWA-OFDM system model is presented in Section 2. The simulation results and analysis are presented in Section 3. Finally, the whole paper is concluded in Section 4.

2 | MODIFIED UWA-OFDM SYSTEM MODEL

At the receiver side, firstly, we are interested to make a time synchronization to obtain the advantages of the OFDM system. We present a time synchronization for UWA wireless communications by using the ZC sequences. The ZC sequences are used in traditional wireless communications as⁴³

$$d_u(k) = \begin{cases} e^{\left\{ -j\pi u \frac{k \times (k+1)}{63} \right\}} & 0 \leq k \leq 30 \\ e^{\left\{ -j\pi u \frac{(k+1)(k+2)}{63} \right\}} & 31 \leq k \leq 61 \end{cases}, \quad (1)$$

where u is the root index of Long-Term Evolution (LTE) standards $u = 25, 29$, and 34 . Select a root index of $u = 25$ for the simulations, as an example.

Figure 1 illustrates the traditional OFDM communication system, while Figure 2 represents the modified OFDM system by using FWHT with LDPC coding. Meanwhile, the MMSE equalizer can be used for ISI elimination with lower complexity using the banded matrix approximation.⁴¹ The transmitting data vector $U(t)$ is generated from the random binary data generator and encoded and then transmitted over the underwater channel. The process of coding is linearly performed. The generator matrix (G) can be obtained from the parity check matrix (H) by using Gauss-Jordan elimination on (H), which is in the form $H = [A, I_{n-k}]$, where A represents $(n-k) \times k$ binary matrix and I_{n-k} is the identity matrix of order $(n-k)$. The dataword of length (k) message bits are encoded to codedword/codedvector of length (n) bits with $n > k$. The codedword/codedvector is generated using generator matrix (G) = $[I_k, A^T]$

$$(V)_{1 \times n} = (U)_{1 \times k} \cdot (G)_{k \times n}, \quad (2)$$

where V , U , and G are the codedword, dataword, and the generator matrix, respectively. If the row space of two matrices G and H are orthogonal, then the generator matrix must satisfy the condition $C H^T = 0$, which indicates that the H matrix is in the symmetric form. The LDPC coding criteria depend on the parity check matrix sparsity. If the sparsity is missed, the required complexity is then of order $\mathcal{O}(N^2)$ operations.³³ Noting that, the FWHT reduces the complexity, which also depends on sparse matrices factorization method. The implementation can be utilized in integrated butterfly structure using Kronecker product technique.⁴² Low complexity implementation of large parity check matrix can be utilized using Reed-Solomon (RS) codes.

According to Figures 1 and 2, the random binary data vectors are multiplied via the generator matrix to obtain the codedword, and after the S/P converter, each symbol is mapped to binary phase shift keying (BPSK) symbols according to the constellation diagram $\bar{S} = [\bar{S}_1, \bar{S}_2, \dots, \bar{S}_N]^T$, where \bar{S} represents the BPSK symbols of length N . In the proposed algorithm illustrated in Figure 2, The N -discrete symbols are implemented via IFWHT, which are define as

$$\{W_N^{-1}\}_{n,i} = \exp\left(-\frac{j2\pi ni}{N}\right), \quad (3)$$

where $n = 0, 1, 2, \dots, N-1$, $i = 0, 1, 2, \dots, N/4-1$.⁴² The output of the FWHT is given by

$$\bar{s} = W_N^{-1} \bar{S}. \quad (4)$$

The ISI can be reduced by using the cyclic prefix (CP) at the head of each OFDM symbol. CP is formed by multiplying the matrix $P = \begin{bmatrix} 0_{N_C \times (N-N_C)}; I_{N_C} \end{bmatrix}^T, I_N^T$. Thus, the encoded data vector resulting from P/S block is transmitted by the hydrophone, which can be expressed as

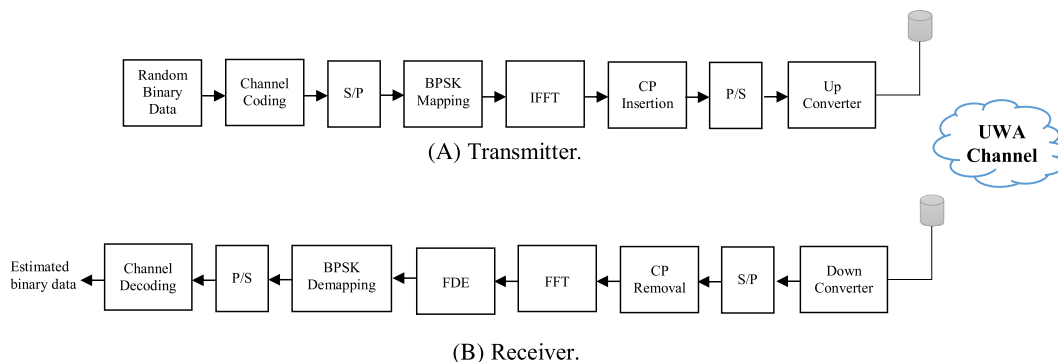


FIGURE 1 Traditional UWA-OFDM communication system

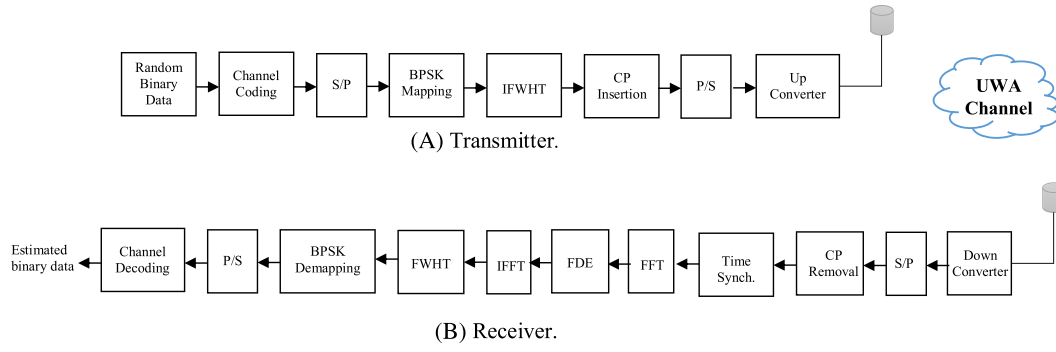


FIGURE 2 Modified UWA-OFDM communication system

$$\bar{s}_{CP} = P \bar{s}. \quad (5)$$

The encoded data vectors are transmitted through the underwater channel and received via the corresponding hydrophone. After CP removal and applying the FFT, the resulting data vector can be expressed as

$$\bar{Y}_1 = F_N(\bar{y}) = I_{m,\bar{m}} \times H \times \bar{s} + N, \quad (6)$$

where $\bar{y} \in \mathbb{C}^{N \times 1}$ is the received vector, $I_{m,\bar{m}}$ is the interference matrix given in Cao et al,⁴¹ H is the transfer function of the UWA channel, $\bar{s} = F_N(\bar{s})$, and N is the additive noise. $F_N(\bar{s})$ denotes the FFT operation of \bar{s} .

Meanwhile, the interference matrix expressed in Equation (5) can be given as⁴¹

$$I_{m,\bar{m}} = \beta \cdot \frac{\sin(\pi[(m - \bar{m}) + \varepsilon])}{N \cdot \sin\left(\frac{\pi[(m - \bar{m}) + \varepsilon]}{N}\right)}, \quad (7)$$

$$\beta = \exp\left(\frac{j\pi[(m - \bar{m}) + \varepsilon](N - 1)}{N}\right), \quad (8)$$

where ε is the normalized CFO describing the relative transmitter and/or receiver motions and $m - \bar{m}$ represents the subcarrier distance. Figure 3 illustrates the amplitude versus the indices of the interference matrix (subcarrier with index 30 is desired); it is clear that the amplitude of the interference matrix is highly decreased as the subcarrier indices

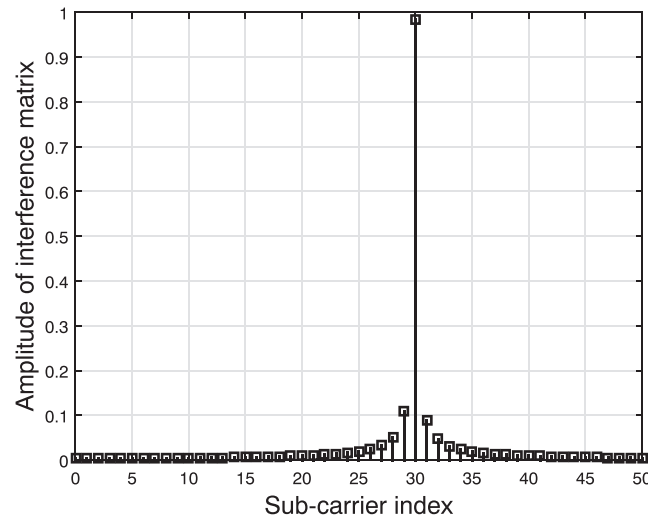


FIGURE 3 Amplitude vs subcarrier index

increased. Thus, a banded matrix BW can be introduced as a design parameter to implement the equalization and the CFO compensation processes with lower complexity.

Now, Equation (6) can be reexpressed as

$$\bar{Y}_1 = \Lambda \times \mathfrak{s} + N. \quad (9)$$

Using the banded matrix approximation,⁴¹ the solutions of the ZF and the MMSE equalizers can perform the equalization and the CFO compensation processes with lower complexity as⁴⁴

$$C_{ZF} = (\psi^H \psi)^{-1} \psi^H, \quad (10)$$

$$C_{MMSE} = \left(\psi^H \psi + \frac{1}{SNR} I_{N \times N} \right)^{-1} \psi^H, \quad (11)$$

where

$$\psi_{m,\bar{m}} = \begin{cases} \Lambda_{m,\bar{m}} & \text{if } |m - \bar{m}| \leq r \\ 0 & \text{if } |m - \bar{m}| > r \end{cases}, \quad (12)$$

where r is the BW of the banded matrix. For simplicity, assuming a ZF equalizer; thus, the output can be given as

$$\bar{Y}_2 = \psi^{-1} \{ \bar{Y}_1 \} = \psi^{-1} \Lambda \mathfrak{s} + \psi^{-1} \cdot N, \quad (13)$$

where $\psi^{-1} \Lambda \approx I_N \times N$. After the IFFT block to remove the effect of the corresponding FFT, Equation (13) can be expressed as

$$\bar{Y}_3 = F_N^{-1} \{ \bar{Y}_2 \} = F_N^{-1} \{ \mathfrak{s} \} + F_N^{-1} \{ \psi^{-1} \cdot N \}, \quad (14)$$

where the $\psi^{-1} \cdot N$ term is the noise enhancement component and $\mathfrak{s} = F_N(\bar{\mathfrak{s}})$; thus Equation (14) can be rewritten as

$$\bar{Y}_4 = \bar{\mathfrak{s}} + F_N^{-1} \{ \psi^{-1} \cdot N \}. \quad (15)$$

Now, after the FWHT block, Equation (15) can be rewritten as

$$\hat{Y} = W_N \{ \bar{Y}_4 \} = \bar{\mathfrak{s}} + \varnothing, \quad (16)$$

where $\varnothing = W_N \{ F_N^{-1} \{ \psi^{-1} \cdot N \} \}$. Thus, we can recover the original transmitted data vector bits; $\bar{\mathfrak{s}}$ represents the transmitted codedworded vector.

2.1 | FWHT-OFDM versus FFT-OFDM system

The modified OFDM system can increase the algorithm speed more than the traditional one, namely, replacing the FFT with FWHT saves about 70% to 36% in computer run-time up to 4096 transform length.⁴² Also, the proposed algorithm has a low implementation cost,⁴² because of lower arithmetic complexity, which builds on the sparse matrices.^{21,45} The IFWHT and FWHT are used instead of IFFT and FFT, at the transmitter and the receiver, respectively. Moreover, in case of UWA communications, the modified OFDM system offers a significant improvement in the BER performance than the corresponding one.^{21,45}

2.2 | The UWA channel model

The main difference between the traditional wireless communication and the corresponding underwater communication is the type of the channel. In underwater communication systems, the signal propagation is affected by many factors such as ambient noise, frequency-dependent attenuation, water temperature, PH degree, and salinity.^{46,47} Moreover, those factors are satisfied to break down the communication among the underwater. On the other hand,

sound signals are used for underwater communication instead of electromagnetic waves because of several reasons such as the electromagnetic waves suffer from large power loss and low effective range.¹ Many researchers are interested in underwater channel modeling,⁴⁸⁻⁵² which helps in the use of signal processing algorithms to predict and improve the real field experiments. Qarabaqi and Stojanovic⁵³ predict and estimate the underwater channel impulse response in case of shallow water. The overall channel transfer function can be expressed as⁵³

$$H(f) = H_o(f) \sum_p h_p \gamma_p(f) e^{-j2\pi f \tau_p} \quad (17)$$

and

$$\gamma_p(f) = \frac{1}{h_p} \sum_{i \geq 0} h_{p,i} e^{-j2\pi f \delta_{\tau_{p,i}}}, \quad (18)$$

where $H(f)$, $H_o(f)$ are the UWA channel transfer function and the transfer function of the direct path, respectively. $\gamma_p(f)$ is the small-scale fading coefficient, and h_p , $h_{p,i}$ are the gain of the intrapath gains of the p th path, respectively. τ_p , $\delta_{\tau_{p,i}}$ are the delay of the intrapath delays of the p th path, respectively.

According to underwater channel parameters given in Table 1, Figure 4 represents the impulse response (IR) of the UWA during a mobile acoustic communications experiment (MACE). The channel showed is a quasi-static channel over single symbol duration.

3 | SIMULATION RESULTS AND ANALYSIS AND COMPLEXITY EVALUATION

3.1 | Simulation results and analysis

This subsection is devoted to performance evaluation of the proposed algorithm via extensive simulation, since the offset in time causes a performance degradation in the OFDM symbol, especially in WHT.⁵⁴ Thus, the STO caused by the underwater channel should be compensated to avoid this problem. Firstly, we have used a ZC sequence for time synchronization. Moreover, in case of UWA-MACE channel, the ZC sequences with root index $u = 25$ can make a time synchronization in the presence of CFO up to $\epsilon = 0.58$.¹⁷ According to the UWA-MACE channel parameters given in Table 1, the OFDM parameters are given in Table 2 and the ZC parameters given in Table 3. Figure 5 shows the planar view of the autocorrelation result of the ZC sequence with the variation of the normalized CFO (ϵ). Also, this figure shows the ability of ZC sequence to specify the starting point of the OFDM symbol in the presence of CFO. Moreover, it is clear that ZC sequences can specify the length of time offsets in the presence of frequency offsets up to $\epsilon \leq 0.58$.¹⁷ After specifying the starting point of the OFDM symbol at the receiver side, an FFT is applied to transfer the received signal to frequency domain to use an FDE. Let us consider an MMSE is used to perform the equalization and CFO compensation processes with lower complexity using banded matrix approximation.⁴¹ Moreover, the complexity of the MMSE equalizer is in order of $48N^3 + \mathcal{O}(N^3)$ flops. On the other hand, using the banded matrix approximation, the complexity of MMSE equalizer can be reduced to $2N(16r^2 + 26r + 5)$ flops. To compensate the effect of the FFT, the corresponding inverse is applied, and then the FWHT is applied. Figure 6 illustrates the performance of the UWA-OFDM based on FFT algorithm with banded matrix approximation and LDPC coding (1024, 512) with $\frac{1}{2}$ rate.

TABLE 1 The UWA-MACE channel parameters

Parameter	Value	Parameter	Value
Channel model	MACE	Central frequency	16 kHz
Water depth	100 m	Surface variance	1.125 m ²
Channel distance	1.00 km	Bottom variance	0.5625 m ²
Transmitter depth	45 m	Number of intrapaths	20
Receiver depth	60 m	Mean of intrapaths	25 mv
Bandwidth of the UWA channel	12 kHz	Variance of intrapaths	1 μ v

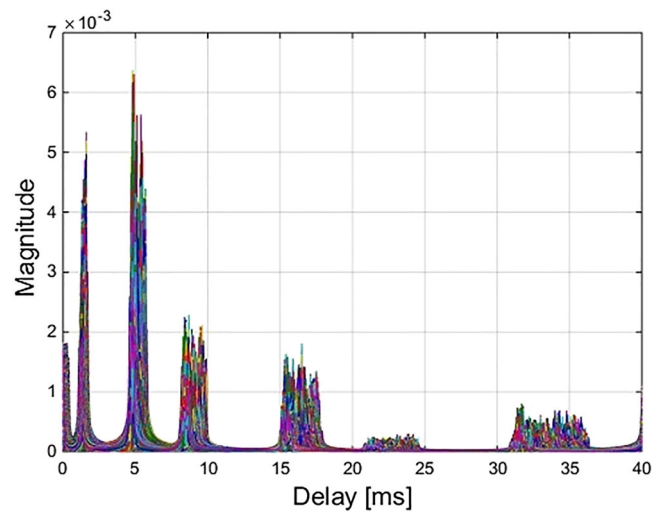


FIGURE 4 The impulse response of underwater acoustic (UWA)–mobile acoustic communications experiment (MACE) channel

TABLE 2 The OFDM parameters

Parameter	Value	Parameter	Value
FWHT/IFWHT size	256	Channel configuration	SISO
FFT/IFFT size	256	Size of the generator matrix	256×512
CP length	16	CFO estimation	Perfect
Modulation	BPSK	Channel estimation	Perfect
SNR	0–20 dB	Channel model	MACE

TABLE 3 The ZC parameters

Parameter	Value	Parameter	Value
ZC length	63	Normalized CFO	$-1.50:0.1:1.50$
Root index of ZC sequence	25	Normalized STO	Zero

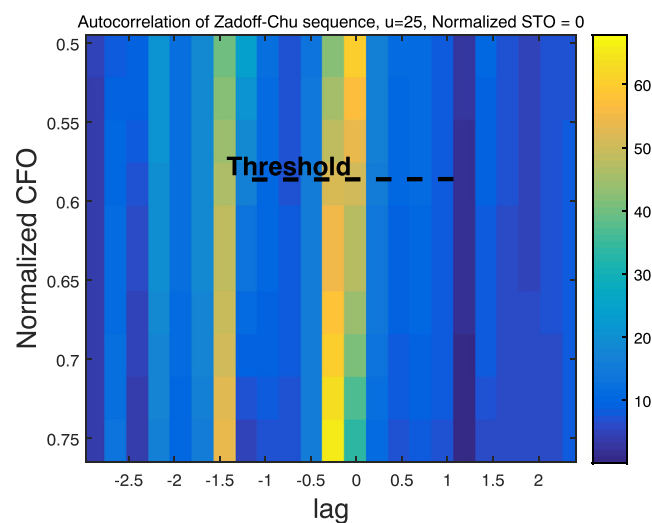


FIGURE 5 The planar view of the autocorrelation results in case of frequency offsets¹⁷

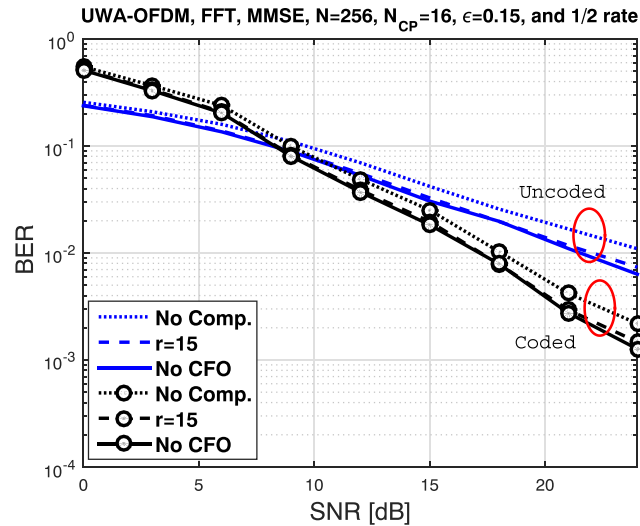


FIGURE 6 Bit-error-rate (BER) vs signal-to-noise ratio (SNR) for underwater acoustic (UWA)-orthogonal frequency division multiplexing (OFDM)-based fast Fourier transform (FFT)

Figure 7 illustrates the performance of the UWA-OFDM based on a FWHT algorithm with banded matrix approximation. According to Figures 6 and 7, it is clear that the performance in case of banded matrix approximation ($r = 15$) is very close to no matrix curve. Figure 8 illustrates the performance of different transforms (FFT and FWHT) with banded matrix approximation and LDPC coding, which shows the important role of the proposed configuration to improve the UWA-OFDM system performance. Also, this figure indicates that the proposed OFDM with FWHT gives a coding gain with mainly 3.46 dB at $\text{BER} = 10^{-3}$. Table 4 gives the different values of the SNR at $\text{BER} = 2 \times 10^{-3}$ of Figures 6 and 7. It is clear that the proposed configuration system lose about 1.00 and 2.02 dB in case of LDPC coding and losses 1.03 and 4.21 dB without coding. These values are obtained with respect to no CFO performance curve. Also, the OFDM based on FFT needs an extra SNR = 8.17 dB to reach the performance of the OFDM based on FWHT with banded matrix approximation ($r = 15$) and LDPC coding. On the other hand, without LDPC coding, the OFDM based on FFT needs an extra SNR more than 7.49 dB to reach the performance of the OFDM based on FWHT with banded matrix approximation ($r = 15$). Table 5 gives the different values of the BER at SNR = 15 dB. It is clear that the BER performance is preserved in case of CFO compensation ($r = 15$) and better performance of the proposed FWHT-OFDM than the corresponding FFT-OFDM system.

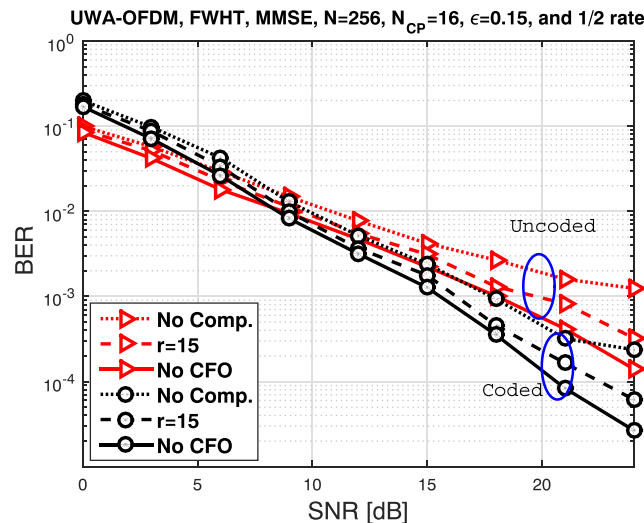


FIGURE 7 Bit-error-rate (BER) vs signal-to-noise ratio (SNR) for underwater acoustic (UWA)-orthogonal frequency division multiplexing (OFDM)-based fast Walsh-Hadamard transform (FWHT)

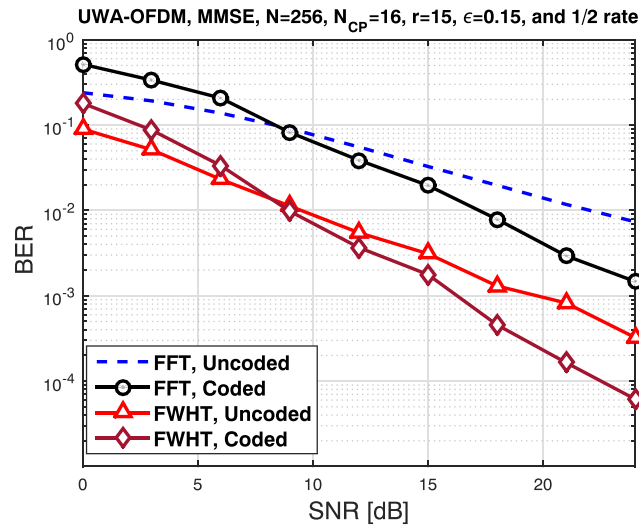


FIGURE 8 Bit-error-rate (BER) vs signal-to-noise ratio (SNR) for underwater acoustic (UWA)-orthogonal frequency division multiplexing (OFDM) with different transforms

TABLE 4 The SNR gain of different transforms of Figures 6 and 7 at $\text{BER} = 2 \times 10^{-3}$

		Proposed Configuration (FWHT)		Traditional Configuration (FFT)	
		SNR, dB	Diff, dB	SNR, dB	Diff, dB
Uncoded	No comp.	19.69	4.21	>24.00	----
	$r = 15$	16.51	1.03	>24.00	----
	No CFO	15.48	0.00	>24.00	----
Coded	No comp.	15.52	2.02	>24.00	>1.78
	$r = 15$	14.50	1.00	22.67	0.45
	No CFO	13.50	0.00	22.22	0.00

TABLE 5 The BER of different transforms at $\text{SNR} = 15$ dB of Figures 6 and 7

		BER	
		Proposed Configuration (FWHT)	Traditional Configuration (FFT)
Uncoded	No comp.	0.004199	0.04193
	$r = 15$	0.003113	0.03273
	No CFO	0.002230	0.03054
Coded	No comp.	0.002394	0.02516
	$r = 15$	0.001775	0.01964
	No CFO	0.001271	0.01833

Figure 9 shows the BER performance of the proposed configuration and the corresponding traditional one at different values of the normalized CFO using the banded matrix approximation ($r = 15$). Table 6 gives the different values of the SNR at $\text{BER} = 2 \times 10^{-3}$, and the case of the FWHT with no CFO is considered as a reference BER performance. It is clear that the proposed OFDM with FWHT improves the system performance than the OFDM-based FFT. Also, increasing the value of the normalized CFO with banded matrix approximation ($r = 15$) leads to more BER performance degradation because of the increase in the amount of the ICI. Table 7 gives the different values of the BER at $\text{SNR} = 15$ dB. It is clear that the BER performance of the OFDM-based FWHT is highly better than the corresponding FFT. Table 7 gives the BER at different conditions of Figure 9 at $\text{SNR} = 15$ dB. This table ensures the important role of the proposed configuration (FWHT) to improve the system performance than the corresponding one (FFT) at different values of the normalized CFO.

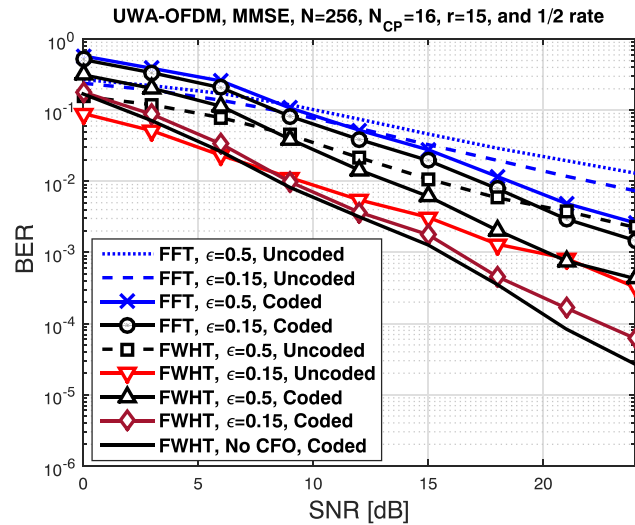


FIGURE 9 Bit-error-rate (BER) vs signal-to-noise ratio (SNR) for underwater acoustic (UWA)-orthogonal frequency division multiplexing (OFDM) with ϵ variation

TABLE 6 The SNR of different transforms at $\text{BER} = 2 \times 10^{-3}$ of Figure 9

Transform Type	Normalized CFO	Coding Status	SNR, dB	Diff., dB
FFT	$\epsilon = 0.5$	Uncoded	>24.00	>10.50
FFT	$\epsilon = 0.15$	Uncoded	>24.00	>10.50
FFT	$\epsilon = 0.5$	Coded	>24.00	>10.50
FFT	$\epsilon = 0.15$	Coded	22.67	9.17
FWHT	$\epsilon = 0.5$	Uncoded	>24.00	>10.50
FWHT	$\epsilon = 0.15$	Uncoded	16.50	3.00
FWHT	$\epsilon = 0.5$	Coded	18.10	4.60
FWHT	$\epsilon = 0.15$	Coded	14.50	1.00
FWHT	No CFO	Coded	13.50	0.00

TABLE 7 The BER of different transforms at $\text{SNR} = 15$ dB of Figure 9

Transform Type	Normalized CFO	Coding Status	BER
FFT	$\epsilon = 0.5$	Uncoded	0.046290
FFT	$\epsilon = 0.15$	Uncoded	0.032730
FFT	$\epsilon = 0.5$	Coded	0.027770
FFT	$\epsilon = 0.15$	Coded	0.019640
FWHT	$\epsilon = 0.5$	Uncoded	0.010780
FWHT	$\epsilon = 0.15$	Uncoded	0.003113
FWHT	$\epsilon = 0.5$	Coded	0.006145
FWHT	$\epsilon = 0.15$	Coded	0.001775
FWHT	No CFO	Coded	0.001271

Figure 10 shows the BER performance of the proposed configuration and the corresponding traditional one in case of estimation errors. It is clear that the proposed system configuration outperforms the corresponding traditional one and gives high fidelity to the BER performance in case of estimation errors. Moreover, the proposed system configuration

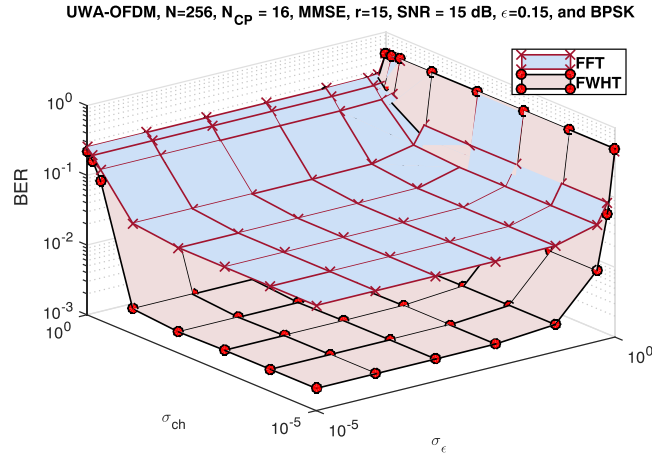


FIGURE 10 The bit-error-rate (BER) of the proposed orthogonal frequency division multiplexing (OFDM)-based fast Walsh-Hadamard transform (FWHT) and the corresponding fast Fourier transform (FFT) in case of estimation errors

TABLE 8 The BER of different transforms using $r = 15$ in case of estimation errors of Figure 10

	$\sigma_{ch} = 0.1, \sigma_{\epsilon} = 10^{-4}$	$\sigma_{ch} = 0.1, \sigma_{\epsilon} = 0.1$	$\sigma_{ch} = 10^{-4}, \sigma_{\epsilon} = 0.1$	$\sigma_{ch} = 10^{-3}, \sigma_{\epsilon} = 10^{-3}$
Proposed configuration	0.038500	0.039210	0.033050	0.032220
Traditional configuration	0.002285	0.002617	0.002457	0.002078

begins to degrade when the standard deviation of the channel estimation errors (σ_{ch}) is more than 0.1, and the standard deviation of the CFO estimation errors (σ_{ϵ}) is more than 0.1. Table 8 gives the corresponding BER value at different values of the standard deviations of the channel and the normalized CFO. Figure 10 and Table 8 give the indication that the proposed MMSE equalizer over the modified OFDM structure can improve and preserve the BER performance in case of estimation errors.

3.2 | Complexity evaluation

This subsection is devoted for the complexity evaluation of the proposed system configuration and compared with the corresponding traditional one. In general, the matrix-matrix multiplications of dimensions $N \times N$ requires approximately N^3 multiplications and N^3 additions for large N .⁵⁵ Matrix-matrix additions of dimensions $N \times N$ requires N^2 additions, matrix inversion of dimensions $N \times N$ requires approximately $O(N^3)$ operations.⁵⁵ Thus, according to Equation (11), the MMSE equalizer needs two matrix-matrix multiplication, matrix inversion, and matrix-matrix additions. This process requires approximately $4N^3 + N^2 + O(N^3)$ operations. Thus, for large size of transmitted data vector,⁴² the computational complexity will be very high. The banded matrix approximation concept is introduced⁴¹ to reduce the computational complexity. According to Cao et al,⁴¹ the matrix-matrix multiplications of dimensions $N \times N$ and $BW = r$ requires approximately $N(2r + 1)^2$ multiplications and $N(2r + 1)^2$ additions. The matrix-matrix addition requires approximately $N(2r + 1)$ additions. The matrix inversion requires approximately $N(2r^2 + 5r + 1)$ operations.⁴¹ On the other hand, the FFT or IFFT algorithm needs $(N/2) \log_2(N)$ multiplications and $N \log_2(N)$ additions.⁵⁶ Thus, the full traditional system requires approximately, $4N^3 + N^2 + O(N^3) + 3N \log_2(N)$ operations. The proposed configuration uses the same structure of the traditional system, in addition to two modifications, the banded matrix approximation, and the addition of IFWHT/FWHT. Assume that the IFWHT requires 70% of the IFFT complexity. Thus, the proposed configuration requires approximately $N(18r^2 + 23r + 6) + 2.7N \log_2(N)$ operations. Hence, the proposed configuration requires a computational complexity $O(N)$ operation, instead of $O(N^3)$ compared with traditional system.

4 | CONCLUSION

In this paper, we propose a modified OFDM system based on WHT with LDPC coding. This algorithm can avoid the errors resulting from time offsets by using the ZC sequences for time synchronization. Under the same conditions of the simulation parameters, the proposed OFDM system with WHT gives better performance than the traditional OFDM system. Also, the proposed MMSE equalizer can perform the equalization and the CFO compensation with lower complexity using banded matrix approximation. Simulation results show that the proposed algorithm with LDPC coding achieved a high fidelity channel communication in case of estimation errors and the variation of the normalized CFO.

REFERENCES

1. Liu SZ, Cui J. Prospects and problems of wireless communications for underwater sensor networks. *Wirel Commun Mobile Comput*. 2008;8:997-994.
2. Ramadan K, Dessouky MI, Elkordy M, Elagooz S, Abd El-Samie FE. Joint low-complexity equalization and carrier frequency offsets compensation for underwater acoustic OFDM communication systems with banded-matrix approximation at different channel conditions. *Int J Commun Syst*. 2018;31(17). <https://doi.org/10.1002/dac.3779>
3. Brekhovskikh LM, Lysanov YP. *Fundamentals of Ocean Acoustics*. second ed. Berlin Heidelberg New York: Springer-Verlag; 1991.
4. Cherubini G, Eleftherious E, Olcer S, Cioffi JM. Filter bank modulation techniques for very high-speed digital subscriber lines. *IEEE Commun Mag*. 2000;38(5):98-104.
5. Amini P, Chen R-R, Farhang-Boroujeny B. Filter bank multicarrier communications for underwater acoustic channels. *IEEE J Oceanic Eng*. 2015;40(1):115-130.
6. Ramadan K, Dessouky MI, Elagooz S, Elkordy M, El-Samie FEA. Equalization and carrier frequency offset compensation for underwater acoustic OFDM systems. *Ann Data Sci J*, Springer. June 2018;5:259-272. DOI: 10.100/s40745-017-0127-y
7. Ramadan K, Fiky AS, Dessouky MI, Abbd-Elsamie FE. Equalization and carrier frequency offset compensation for UWA-OFDM communication systems based on the discrete sine transform. *Digital Signal Process, Elsevier*. 2019. <https://doi.org/10.1016/j.dsp.2019.02.004>
8. Xing S, Qiao G, Ma L. A blind side information detection method for partial transmitted sequence peak-to-average power reduction scheme in OFDM underwater acoustic communication system. *IEEE Access*. 2018;6:24128-24136.
9. Cho YS, Kim J, Yang WY, Kang CG. *MIMO-OFDM Wireless Communications with MATLAB*. Asia: John Wiley & Sons, IEEE Press; 2010:153-161.
10. Subba B, Visuvanathan GE. PAPR reduction using SC-FDMA in underwater acoustic channel. *Int J Appl Eng Res*. 2017;12:1793-1797.
11. Kumar P, Kumar P. "Performance evaluation of DFT-spread OFDM and DCT-spread OFDM for underwater acoustic communication. In: 2012 IEEE Vehicular Technology Conference (VTC Fall), India, 2012.
12. Li B, Zhou S, Stojanovic M, Freitag L, Willett P. Non-uniform Doppler compensation for zero-padded OFDM over fast-varying underwater acoustic channel. In: Proc. of MTS/IEEE OCEANS conference, Aberdeen, Scotland, 2007.
13. Cheng X, Wen M, Cheng X, Yang L. Effective self-cancellation of inter carrier interference for OFDM underwater acoustic communications. In: Proceedings of the International Conference on Under Water Networks and Systems (WUWNet), Kaohsiung, Taiwan, Nov. 2013.
14. Trivedi VK, Ramadan K, Kumar P, Dessouky MI, El-Samie FEA. Enhanced OFDM-NOMA for next generation wireless communication: a study of PAPR reduction and sensitivity to CFO and estimation errors. *AEU Int J Electron Commun*. Jan 2019, <https://doi.org/10.1016/j.aeue.2019.01.009>;102:9-24.
15. Mashdour S, Jamshidi A. Multiple CFO estimation in OFDM underwater communication systems. *Trans Electr Eng*. 2014;38:137-148.
16. Bi Y, He Z, Jiang W, Niu K, Rong Y. Design and experiment of frequency offset estimation and compensation in high-speed underwater acoustic communication. In: 2015 International Conference on Wireless Communications & Signal Processing (WCSP), Nanjing, China, 2015.
17. Ramadan K, Dessouky MI, Elagooz S, Elkordy M, Abd El-Samie FE. Carrier frequency offsets estimation in UWA-OFDM communication systems using Zadoff-Chu sequences. *Int J Electron Lett, Taylor&Francis*. 2018;7(2):127-142. <https://doi.org/10.1080/21681724.2018.1461249>.
18. Ramadan K, Ramadan KF, Fiky AS, Alam H, Dessouky MI, El-Samie FEA. Joint low-complexity equalization and CFO estimation and compensation for UWA-OFDM communication systems. *Int J Commun Syst*. 2019. <https://doi.org/10.1002/dac.3972>
19. Ramadan K, Dessouky MI, Abd-Elamie FE. Equalization and blind CFO estimation for performance enhancement of OFDM communication systems using discrete cosine transform. *Int J Commun Syst*, Wiley, IJCS-18-0061.R1. 2019. <https://doi.org/10.1002/dac.3984>
20. Chen H, Liang H. Binary Golay complementary sequences in Walsh-Hadamard transformed OFDM systems. In: 2006 International Symposium on Intelligent Signal Processing and Communications, ISPACS'06, 2007: 999-1002.
21. Kumar P, Kumar P. Performance evaluation of modified OFDM for underwater communications. In: IEEE international conference on communications, 2013.

22. Moshavi S. Multi-user detection for DS-CDMA communications. *IEEE Communications Magazine*. 1996;34:124-136. <https://doi.org/10.1109/35.544334>
23. Yang TC, Yang WB. Interference suppression for code division multiple access communications in underwater acoustic channel. *J Acoust Soc Am*. 2009;126(1):220-228. <https://doi.org/10.1121/1.3147484>
24. Tuchler M, Koetter R, Singer A. Turbo equalization: principles and new results. *IEEE Trans Commun*. 2002;50(5):754-767.
25. Tuchler M, Singer A. Turbo equalization: an overview. *IEEE Trans Inf Theory*. 2011;57(2):920-952.
26. Berrou C, Glavieux A. Near optimum error correcting coding and decoding: turbo-codes. *IEEE Trans Commun*. 1996;44(10):1261-1271.
27. Yang TC. Properties of underwater acoustic communication channels in shallow water. *J Acoust Soc Am*. 2012;131(1):129-145. <https://doi.org/10.1121/1.3664053>.
28. Kang T, Song HC, Hodgkiss WS, Soo Kim J. Long-range multi-carrier acoustic communications in shallow water based on iterative sparse channel estimation. *J Acoust Soc am*. 2010;128(6):EL372-EL377.
29. Zhang J, Zheng Y. Frequency-domain turbo equalization with soft successive interference cancellation for single carrier MIMO underwater acoustic communications. *IEEE Trans Wireless Commun*. 2011;10(9):2872-2882.
30. Tao J, Zheng Y. Turbo detection for MIMO-OFDM underwater acoustic communications. *Int J Wireless Inf Netw*. 2013;20(1):27-38.
31. Zhang L, X X, Feng W, Chen Y. Multi-array iterative receiver for underwater acoustic OFDM communications with EXIT chart evaluation. *Appl Acoust*. 2016;114:307-316.
32. Han W, Huang J, Jiang M. Performance analysis of underwater digital speech communication system based on LDPC codes. In: Industrial Electronica and Applications (ICIEA), IEEE 4th International Conference, 2009.
33. Chen Y, Xu X, Zhang L. Performance analysis of LDPC codes over shallow water acoustic channels. In: 5th International Conference on Wireless Communications, Networking and Mobile Computing, 2009.
34. Gallager R. Low density parity check codes. *IRE Trans Info Theory*. 1962;8(1):21-28.
35. Gallager RG. *Low density parity check codes*. Cambridge: MIT Press; 1963.
36. Zheng YR, Xiao C, Yang TC, Yang W-B. Frequency-domain channel estimation and equalization for shallow-water acoustic communications. *Phys Commun*. 2010;3(1):48-63.
37. Al-Kamali FS, Dessouky MI, Sallam BM, Shawki F, Al-Hanafy W, Abd El-Samie FE. Joint low-complexity equalization and carrier frequency offsets compensation scheme for MIMO SC-FDMA systems. *IEEE Trans Wirel Commun*. 2012;11(3):869-873.
38. Huang JZ, Zhou S, Huang J, Berger CR, Willett P. Progressive inter-carrier interference equalization for OFDM transmission over time-varying underwater acoustic channels. *IEEE J Sel Top Sign Proces*. Dec. 2011;5(8):1524-1536.
39. Choi JW, Drost RJ, Singer AC, Preisig J. Iterative multi-channel equalization and decoding for high frequency underwater acoustic communications. In: Proceedings of the 5th IEEE Sensor Array and Multichannel Signal Processing Workshop, July 2008.
40. Ramadan K, Dessouky MI, Abd-Elsamie FE, Elagooz S. Virtual quadrature phase shift keying with low-complexity equalization for performance enhancement of OFDM systems. *Int J Electron Commun*. 2018;96:199-206. <https://doi.org/10.1016/j.aeue.2018.08.031>
41. Cao Z, Tureli U, Yao Y. Low-complexity orthogonal spectral signal construction for generalized OFDMA uplink with frequency synchronization errors. *IEEE Trans Vehic Tech*. May 2007;56(3):1143-1154.
42. Hamood M, Boussakta s. Fast Walsh-Hadamard-Fourier transform. *IEEE Trans Signal Process*. November 2011;59:5626-5673.
43. Wang D, Shi W, Li X. Low-complexity carrier frequency offset estimation algorithm in TD-LTE. *J Networks*. Oct. 2013;8(10).
44. Tao J, Rosa Zheng Y, Xiao C, Yang TC, Yang W-B. Channel equalization for single carrier MIMO underwater acoustic communications. *EURASIP J Adv Signal Process*. 2010;2010(1).
45. Ding H, Neasham JA, Boussakta S. Performance evaluation of T-transform based OFDM in underwater acoustic communications. In: *OCEANS 2015 - Genova*, Genoa, Italy, 21 September 2015.
46. Francois RE, Garrison GR. Sound absorption based on ocean measurements: part I: pure water and magnesium sulfate contributions. *J Acoust Soc am*. 1982;72(3):896-907.
47. Francois RE, Garrison GR. Sound absorption based on ocean measurements: part II: boric acid contribution and equation for total absorption. *J Acoust Soc am*. 1982;72(6):1879-1890.
48. Chitre M. A high-frequency warm shallow water acoustic communications channel model and measurements. *J Acoust Soc Amer*. 2007;122(5):2580-2586.
49. Socheleau F, Passerieux J, Laot C. Characterisation of time varying underwater acoustic communication channel with application to channel capacity. In: presented at the Underwater Acoust. Meas. Conf., Nafplion, Greece, Jun. 2009.
50. Qarabaqi P, Stojanovic M. Statistical modeling of a shallow water acoustic communication channel. In: Proc. Underwater Acoust. Meas. Conf., Nafplion., Greece, Jun. 2009.
51. Radosevic A, Proakis J, Stojanovic M. Statistical characterization and capacity of shallow water acoustic channels. In: in Proc. IEEE OCEANS Eur. Conf., 2009.
52. Yang WB, Yang TC. High-frequency channel characterization for M-ary frequency-shift-keying underwater acoustic communications. *J Acoust Soc Amer*. 2006;120(5):2615-2626.

53. Qarabagi P, Stojanovic M. Statistical characterization and computationally efficient modeling of a class of underwater acoustic communication channels. *IEEE J Oceanic Eng.* Oct. 2013;38(Special):701-717.
54. Ahmed MSh., Al-iesawi SA. Efficient Joint carrier offset and channel estimator for T-OFDM system. In: The First International Conference of Electrical, Communication, Computer, Power and Control Engineering, Iraq, 2013.
55. Golub H, Van Loan CF. *Matrix Computations*. 3rd ed. Baltimore, MD, USA: Johns Hopkins University Press; 1996.
56. Cooley JW. The re-discovery of the fast Fourier transform algorithm. *Mikrochimica Acta, Springer Verlag*. 1987;3:33-45.

How to cite this article: El-Mahallawy M, Eldien AT. Performance enhancement of UWA-OFDM communication systems based on FWHT. *Int J Commun Syst.* 2019;32:e3979. <https://doi.org/10.1002/dac.3979>